# Supporting Information

## Supplemental Materials and Methods

**Plasmid Construction.** To isolate Cep192-binding proteins, a *Pme*I-*Not*I fragment containing the cDNA of the gene of interest was generated by RT-PCR using SuperScript III RT (Invitrogen), and then cloned into a pCI-neo-$FLAG_3$ vector (pKM2795) digested by the corresponding enzymes. pCI-neo-$FLAG_3$–based constructs containing the full-length (pKM3445), N (pKM3506), C (pKM3507), CPB (pKM3508), or PB (pKM3509) of Plk4 were generated in a manner similar to what is described above by inserting each respective *Pme*I-*Not*I fragment into the pCI-neo-$FLAG_3$ vector. The pCI-neo-Plk4 (no tag) construct (pKM3681) was generated by digesting pKM3445 with *Asc*I (end-filled) and *Pme*I, and self-ligating the resulting fragment. The pEGFP-C2-Cep192 (pKM3105) construct encoding residues 1–2538 of Cep192 was generated by inserting an RT-PCR-generated N-terminal fragment of Cep192 into the pCR3.1-EGFP-Cep192 (507–2538) construct (a gift of David Sharp, Albert Einstein College of Medicine, Bronx, NY). To obtain the pEGFP-C1-Cep192 WT (pKM3552), D214A (pKM3897), D216A (pKM3881), or D214A D216A (pKM3815) construct, a *Sal*I fragment containing the respective fragment was subcloned into the pEGFP-C1 vector (Clontech) digested by the corresponding enzyme.

For the construction of Cep192 deletion mutants, a *Sal*I fragment containing Cep192 (1–647) (pKM3290) or Cep192 (1700–2538) (pKM3289), or a *Pme*I/*Sma*I fragment containing Cep192 (901–1800) (pKM3288) was cloned into the pEGFP-C1 vector digested by either *Sal*I or *Sma*I, respectively. The Cep192 (507–1065) construct

(pKM3114) was generated by self-ligating the pCR3.1-EGFP-Cep192 (507–2538) construct after digesting it with *Eco*RV and *Apa*I (end filled).

To generate serial deletion constructs from pEGFP-C1-Cep192 (1–647), a *Sal*I-*Sma*I fragment containing Cep192 (1–110) (pKM3374), Cep192 (101–210) (pKM3375), Cep192 (201–310) (pKM3376), Cep192 (301–410) (pKM3377), Cep192 (401–510) (pKM3378), Cep192 (401–647) (pKM3379), or Cep192 (501–647) (pKM3380), was inserted into the pEGFP-C1 vector digested by the same enzymes. Another set of serial deletion constructs was generated from the N- or C-terminus of pEGFP-C1-Cep192 (201–310) (pKM3376) similarly as above. The inserts are a *Sal*I-*Sma*I fragment of Cep192 (210–310) (pKM3495), Cep192 (220–310) (pKM3496), Cep192 (230–310) (pKM3497), Cep192 (240–310) (pKM3498), or Cep192 (250–310) (pKM3499) from the N-terminus of the full-length Cep192, or Cep192 (201–300) (pKM3510), Cep192 (201–290) (pKM3511), Cep192 (201–280) (pKM3512), Cep192 (201–270) (pKM3513), or Cep192 (201–260) (pKM3514) from the C-terminus of the full-length Cep192.

All the pEGFP-C1-Cep192 (201–280) (i.e., Cep192 DN80 for simplicity)-based mutants were generated by inserting a PCR-mutagenized *Sal*I-*Sma*I fragment into the pEGFP-C1 vector digested by the respective enzymes. The introduced mutations are E210A (pKM3532), D211A (pKM3543), D214A (pKM3525), D215A (pKM3526), D216A (pKM3527), D218A (pKM3528), D219A (pKM3529) and E220A (pKM3533) from the acidic-α-helix motif, and K252A (pKM3534), K255A (pKM3535), N259A (pKM3536), Q263A (pKM3537), N267A (pKM3538), N271A (pKM3539), Q275A (pKM3540), and N279A (pKM3541) from the N/Q-rich motif.

The human Cep152 full-length cDNA was PCR amplified from an MGC human clone (ID 40125733, Open Biosystems). An *Xho*I-*Sma*I fragment was cloned into the pEGFP-C1 vector digested by the same enzymes to generate the pKM3841 construct. The pEGFP-C1-Cep152 (D43A) (pKM3848), -Cep152 (D44A) (pKM3849), and -Cep152 (D43A D44A) (pKM3850) constructs were generated by inserting the respective *Xho*I-*Hind*III fragment into the pEGFP-C1 vector digested by the corresponding enzymes.

To construct pEGFP-C1-Cep152 (1–217) (i.e., Cep152 DN217 for simplicity) WT (pKM3561) or mutants, a *Sal*I-*Sma*I fragment was inserted into the pEGFP-C1 vector digested by the same enzymes. The mutations introduced are D40A (pKM3769), D43A (pKM3770), D44A (pKM3771), D45A (pKM3772), L46A (pKM3773), E50A (pKM3774), L51A (pKM3775), Y53A (pKM3776), and D55A (pKM3777). GFP-tagged Cep152 deletion constructs, containing residues 27–180 (pKM3542), 1–217 (pKM3561) or 1–512 (pKM3562), were created by inserting each respective *Sal*I-*Sma*I fragment into the pEGFP-C1 vector digested by the corresponding enzymes.

To generate pCI-neo-$FLAG_3$-Cep192 (pKM4199) and pCI-neo-$FLAG_3$-Cep152 (pKM2809), a *Pme*I-*Not*I fragment of Cep192 from pEGFP-C1-Cep192 and an *Xho*I-*Sma*I fragment of Cep152 PCR products were subcloned into a pCI-neo-$FLAG_3$ vector digested by *Pme*I and *Not*I for the former construct, and digested by *Xho*I and *Sma*I for the latter construct.

To generate a GST-fused mammalian construct expressing Cep192 DN80 (pKM3767) or Cep152 DN217 (pKM4085), a *Xho*I-*Sma*I fragment from pEGFP-C1-Cep192 DN80 (pKM3512) or pEGFP-C1-Cep152 DN217 (pKM3561), respectively, was

cloned into a pCI-neo-GST vector (a CI-neo-$FLAG_3$ variant that has a GST in replacement of $FLAG_3$) (pKM3754) digested by the same enzymes. Their respective 2A mutants, pCI-neo-GST-Cep192 DN80 (D214A D216A) (pKM4112) and pCI-neo-GST-Cep152 DN217 (D43A D44A) (pKM4086), were generated by PCR mutagenesis.

The pcDNA3.1-HA-Sas6 and pcDNA3.1-HA-Cep135 constructs were kindly provided by Kunsoo Rhee (Seoul National University, Seoul, South Korea). For the construction of pCI-neo-$FLAG_3$-Cep135 (pKM4419), a *Sma*I-*Xho*I fragment prepared from pcDNA3.1-HA-Cep135 was subcloned into the pCI-neo-$FLAG_3$ vector digested by *Pme*I and *Xho* I enzymes.

The lentiviral constructs, pHR′.J-CMV-Cep192 WT (pKM3235) and its 2A mutant (pKM4323), were cloned by inserting the respective *Sal*I fragment into a pHR′.J-CMV-SV-puro vector (pKM2994) digested by the same enzyme. The pHR′.J-CMV-Cep152 WT (pKM4325) and its 2A mutant (pKM4327) were generated by inserting the respective *Xho*I (end-filled)-*Sma*I fragment into a pHR′.J-CMV-SV-puro vector digested by *Sma*I.

The lentiviral constructs expressing GFP-Cep192 DN80 WT (pKM4246) or 2A mutant (pKM4249) and GFP-Cep152 DN217 WT (pKM4248) or 2A mutant (pKM4247) were generated by inserting each respective *Asc*I-*Bam*HI fragment into the pHR′.J-CMV-SV-puro vector digested by the corresponding enzymes. A pHR′-CMV-SV-puro-GFP (pKM1992) was constructed by inserting an *Age*I (end-filled)-*Eco*RV fragment containing the GFP ORF into a pHR′-CMV-SV-puro vector digested by *Bam*HI (end filled).

For generating lentivirus-based shRNA constructs, each annealed oligonucleotide fragment was inserted into a pLKO.1-puro vector (a gift from S.A. Stewart and P.A. Sharp, MIT, Cambridge, MA) digested by *Age*I and *Eco*RI. All the target sequences for lentivirus-based shRNAs and synthetic siRNAs are summarized in Table S1.

To generate genes bearing silent mutations against shRNA/siRNA-based gene silencing, several nucleotide mutations were introduced by PCR-based mutagenesis. To generate a Cep192-sil mutant resistant to siCep192 treatment, PCR-based mutagenesis was carried out using a forward oligo (5′-GC**A**AG**A**ATGTC**A**GA**C**AC**A**TGG-3′; nucleotides 2407–2427). To create a Cep152-sil mutant refractory to siCep152 treatment, two independent regions of the Cep152 open-reading frame were mutated with one forward oligo (5′-GG**A**TT**A**GA**G**CC**C**TATAATA-3′; nucleotides 556–574) and the other forward oligo (5′-GCG**T**AT**T**CA**G**CT**T**GAAATCTA-3′; nucleotides 3099–4019). Silent mutations are indicated in boldface type.

**Sequence Comparison and Secondary Structure Prediction.** Comparative sequence analyses were performed using the NCBI blast program. The PredictProtein program was used to predict secondary structures, including the α-helix.

**Tandem Affinity Purification of Cep192-Binding Proteins.** To isolate Cep192-binding proteins, HeLa cells stably expressing ZZ-TEV-$FLAG_3$-Cep192 were generated with a lentiviral expression system. Cell pellets were washed with cold PBS, and lysed in a TBSN buffer [20 mM Tris-Cl (pH 8.0), 150 mM NaCl, 0.5% Nonidet P-40, 5 mM EGTA, 1.5 mM EDTA, 20 mM p-nitrophenylphosphate and protease inhibitor cocktail

(Roche)] (1). After centrifugation at 15,000 x *g* for 20 min, the resulting supernatant was incubated with IgG beads (GE Healthcare) for 2 h at 4°C. After washing, the beads were treated with TEV protease for 6 h at 4 °C to elute Cep192 and its binding proteins (first purification). The eluate was then immunoprecipitated with bead-immobilized anti-FLAG antibody (Sigma), and washed, and the immunoprecipitates were incubated with the 3xFLAG peptide to elute the $FLAG_3$-Cep192 and its associated proteins (second purification). The final eluate was resolved by SDS-PAGE, and then subjected to mass spectrometry analysis.

**Cell Culture and Transfection.** U2OS and 293T cells were cultured as recommended by the American Type Culture Collection. Where indicated, cells were treated with 2.5 mM thymidine (Sigma) or 200 nM nocodazole (Sigma) for 20 h to trap the cells in the S phase or prometaphase, respectively. Transfection was carried out using either Lipofectamine 2000 (Invitrogen) for protein overexpression or Lipofectamine RNAiMAX (Invitrogen) for siRNA transfection. To effectively deplete Cep192 or Cep152 proteins, U2OS cells were transfected twice with siRNA against control Luciferase (siGL), Cep192 (siCep192), or Cep152 (siCep152) for the total period of 96 h.

**Lentivirus Production, Infection, and Generation of Stable Cell Lines.** Lentiviruses expressing various proteins were generated by cotransfecting 293T cells with pHR′-CMVΔR8.2Δvpr, pHR′-CMV-VSV-G (protein G of vesicular stomatitis virus), and pHR'-CMV-SV-puro-based constructs containing a gene of interest, using the $CaCl_2$ transfection method that was previously described (2). Various stable U2OS cell lines

were generated by infecting the cells with lentiviruses expressing the gene of interest, and selecting the cells with 2 μg/ml of puromycin (Sigma). The resulting cells were then transfected two times with various siRNAs to deplete the RNAi-sensitive respective endogenous proteins. See Fig. S10 for the detailed experimental procedure.

**Immunoprecipitation and Immunoblotting Analyses.** For immunoprecipitation, cells were lysed in TBSN buffer (see above), and immunoprecipitation was carried out as previously described (1). Immunoprecipitated proteins were separated by 10% SDS-PAGE (7% to detect Cep192 and Cep152), transferred to a PVDF membrane, and then detected by immunoblotting with indicated antibodies using an enhanced chemiluminescence (ECL) detection system (Pierce).

The quantification of the results shown in Fig. 2 was performed by measuring the intensities of the signal using Image J and then calculating the levels of the inter- or intra-molecular interactions between Cep192 and Cep152 relative to that of the Cep192-Plk4 interaction. For instance, since Cep192 immunoprecipitation with an anti-GFP antibody co-precipitates both Plk4 and Cep192 (the eighth lane), the relative amount of Plk4 co-precipitated from the given Plk4 input amount was considered 1.00. Compared to this co-precipitation efficiency (1.00), the relative efficiency of co-precipitating Cep192 was calculated to be 60% of that of the Cep192-Plk4 interaction (0.18/0.30 = 0.60). Using this proportional calculation method, we estimated that the efficiency of the Cep152-Cep152 interaction is ~54% of that of the Cep152-Plk4 interaction. The level of the interaction between Cep192 and Cep152 was negligible (less than ~2%).

**Indirect Immunofluorescence Microscopy and Quantification.** Immunostaining analysis was carried out essentially as previously described (3) using antibodies against Cep192, Cep152, Plk4, Sas6 (Santa cruz), or Centrin (Millipore). All the appropriate secondary antibodies were used for immunostaining. Alexa Fluor 488 (green)-conjugated anti-Cep192 (rabbit) or anti-Cep152 (rabbit) antibody was used to avoid cross-reactivities with another rabbit antibody. To visualize chromosomes, cells were treated with PBS containing 0.1 μg/ml of 4′,6′-diamidino-2- phenylindole (DAPI) (Sigma). Confocal images were obtained using the Zeiss LSM 780 system mounted on a Zeiss Observer Z1 microscope. To quantify the fluorescence signal intensities, images of unsaturated fluorescence signals were acquired with the same laser intensity at 512 x 512 pixels and 12-bit resolution. Intensities of fluorescence signals were quantified using Zeiss ZEN confocal software, and then plotted using GraphPad Prism 6 program.

## Supplemental Figure Legends

**Fig. S1.** Isolation of Plk4 as a Cep192-binding protein. *(A)* To isolate Cep192-binding proteins, HeLa cell lysates expressing ZZ-TEV-$FLAG_3$-Cep192 were subjected to immunoglobulin G (IgG)-affinity purification (the ZZ tag is a derivative of the *Staphylococcus* protein A that has a high affinity to IgG). After TEV (a highly site-specific protease found in the tobacco etch virus) digestion, $FLAG_3$-Cep192 was eluted from the ZZ beads and immunoprecipitated with anti-FLAG antibody. The immunoprecipitates were then incubated with FLAG epitope peptide to elute $FLAG_3$-Cep192 and its associated proteins. The resulting eluate was analyzed by mass spectrometry to identify potential Cep192-binding proteins. To confirm the interaction between Cep192 and its potential binding candidates, 293T cells cotransfected with the indicated constructs were subjected to co-immunoprecipitation analyses. Among the various candidates tested, Plk4 appeared to be the only one that efficiently interacted with Cep192. In, 1% input; IP, immunoprecipitation; Arrowhead, co-immunoprecipitated Plk4. *(B)* 293T cells cotransfected with the indicated constructs were treated with either thymidine (Thy) or nocodazole (Noc) for 20 h. Total lysates were prepared and subjected to co-immunoprecipitation analyses. The middle part of the anti-GFP panel is deleted (dotted line) to save space.

**Fig. S2.** Deletion analyses to identify the Plk4-binding region in Cep192. *(A)* To determine the region of Cep192 that is critically required for Plk4 binding, 293T cells were transfected with the full-length $FLAG_3$-Plk4 and various, GFP-fused, truncated

forms of Cep192 (left), and then immunoprecipitated (right). Numbers indicate amino acid residues. Note that Cep192 (1–647) that binds to Plk4 also stabilizes the latter in the input. It is possible that Cep192 stabilizes Plk4 by either inhibiting its autophosphorylation activity or disrupting its interaction with SCF-β-TrCP. *(B* and *C)* The Cep192 (1–647) fragment that binds to Plk4 in *(A)* was subjected to subsequent deletion analyses. The results show that the Cep192 (201–280) fragment, called DN80 (an 80 residue-long fragment containing acidic-α-helix and N/Q-rich motifs), is fully capable of binding to Plk4. Asterisk in *(A* and *C)*, nonspecific cross-reacting proteins; asterisk in *(B)*, a remaining anti-FLAG signal from a previous immunoblot; arrowheads in (*B* and *C*), various GFP-Cep192 fragments immunoprecipitated by the anti-GFP antibody.

**Fig. S3.** The CPB of Plk4 binds to Cep192 (201–310) or Cep192 (201–280). *(A* and *B)* 293T cells transfected with various truncated forms of Plk4 and GFP-fused Cep192 (201–310) were subjected to reciprocal co-immunoprecipitation analyses with either the anti-GFP *(A)* or anti-FLAG *(B)* antibody. The immunoprecipitates were immunoblotted with the indicated antibodies. Results showed that CPB is sufficient to interact with Cep192. Arrowheads mark the positions of Plk4 full-length and deletion forms. *(C)* 293T cells transfected with GFP-Cep192 (201–280) (i.e., DN80) and various forms of Plk4 were subjected to co-immunoprecipitation analyses. Arrowheads, the positions of Plk4 full-length and deletion forms; asterisk in *(A)*, cross-reacting protein; asterisks in *(C),* remaining anti-FLAG signals originated from a previous immunoblot.

**Fig. S4.** Mutational analyses of the C-terminus N/Q-rich motif of Cep192 DN80 for Plk4 binding. 293T cells cotransfected with $FLAG_3$-Plk4 CPB and the indicated DN80 point mutants were subjected to co-immunoprecipitation analyses. Results showed that the N259A mutation significantly crippled the DN80-CPB interaction, while the K255A and Q275A mutations moderately diminished it. Numbers, relative levels of co-immunoprecipitated Plk4 CPB.

**Fig. S5.** Interaction analyses between Plk4 and Cep152 and between Cep192 and Cep152. *(A* and *B)* 293T cells were cotransfected with various GFP-fused N-terminal fragments of Cep152 and either full-length $FLAG_3$-Plk4 *(A)* or $FLAG_3$-Plk4 CPB *(B)*. The resulting cells were harvested and subjected to co-immunoprecipitation analyses. Cep192 DN80 that efficiently binds to Plk4 was included for comparison. Note that the Cep192- and Cep152-truncated constructs that interact with the full-length Plk4 in *(A)* also stabilize Plk4 in the input. Arrowheads in (*A* and *B*), immunoprecipitated GFP-Cep192 and GFP-Cep152 fragments. *(C)* 293T cells transfected with the indicated constructs were subjected to coimmunoprecipitation (IP) analysis. To diminish a potential steric hindrance with GFP-tagged constructs in Fig. 2D, HA-tagged Cep152, $FLAG_3$-tagged Cep192, and untagged Plk4 were used. "-" indicates control vector. Note that immunoprecipitation of $FLAG_3$-Cep192 failed to detectably coimmunoprecipitate Cep152 under our buffer conditions containing 150 mM NaCl. Under the same conditions, Plk4 was efficiently coimmunoprecipitated.

**Fig. S6.** Characterization of an anti-Plk4 antibody generated against its C-terminal region. *(A)* Total cellular lysates were prepared from 293T cells transfected with the indicated constructs. Total protein samples were separated by 10% SDS-PAGE and subjected to immunoblotting analysis with a rabbit antibody generated against the C-terminal region (residues 580–970) of Plk4 (left). The same lysates were subjected to anti-FLAG immunoblotting for comparison (right). Asterisks, cross-reacting proteins. N, Plk4 (1–581); C, Plk4 (580–970). *(B)* U2OS cells were silenced for either control luciferase (shGL) or Plk4 (shPlk4) using a lentiviral RNAi system, and then immunostained with the indicated antibodies. Note that Plk4 signals disappeared after shPlk4 treatment, whereas Centrin signals remained at similar levels. *(C)* Asynchronously growing U2OS cells were coimmunostained with the anti-Plk4 antibody used in *(A)* and an anti-Centrin antibody. Consistent with its role in centriole duplication, Plk4 was abundant at G1 and S centrosomes but was scarce at M phase centrosomes.

**Fig. S7.** Subcentrosomal localization patterns of Plk4 at the early stages of the cell cycle. Asynchronously growing HeLa cells stably expressing Centrin2-GFP were immunostained with the anti-Plk4 antibody described in Fig. S6. Samples were then subjected to 3D-SIM analyses. Images show cells with either unduplicated (single) or duplicated centrioles (duplicated) per centrosome. Note that in the cells with duplicated centrioles, Plk4 dot signals are closely located to two nascent Centrin signals (two smaller green dot signals in the fifth and sixth panels) at procentrioles.

**Fig. S8.** Subcentrosomal localization patterns of Plk4, Cep192, and Cep152. *(A)* U2OS cells were co-stained with anti-Plk4 (rabbit) and anti-Sas6 (mouse) antibodies, followed by an additional staining with an Alexa 488-conjugated anti-Cep192 (rabbit) antibody. Samples were analyzed using 3D-SIM. The localization patterns of Plk4 were similar to those shown in Fig. 4*A–C.* It was apparent that Cep192 localizes to both mother and daughter centrioles from early in the cell cycle. Plk4 appeared to colocalize with only a part of cylindrical Cep192 signals. Cep192 signals became significantly larger in size at the late stages of the cell cycle, suggesting that the level of Cep192 increases as PCM expands at these stages. *(B)* Immunostaining of U2OS cells was carried out as described in *(A)*, except that an Alexa 488-conjugated anti-Cep152 (rabbit) antibody was used. Arrows indicate that Plk4 is fully recruited to daughter centrioles, while Cep152 is not. Note that Plk4 was colocalized with only a fraction of the Cep152 toroid.

**Fig. S9.** Both Cep192 and Cep152 are required for proper centriole biogenesis. *(A–E)* To examine the effect of the depletion of Cep192 or Cep152 on the levels of Plk4 and Sas6 at centrosomes, U2OS cells were silenced for either control luciferase (siGL), Cep192 (siCep192), Cep152 (siCep152), or both Cep192 and Cep152 (siCep192 siCep152). Four days after transfection (two times with a two-day interval), a fraction of these cells were subjected to immunoblotting *(A)* analysis. The membranes were stained with Coomassie (CBB) for loading controls. The remaining cells were subjected to immunostaining analyses *(B)* to quantify the level of centrosomally localized Plk4 and the fraction of cells with detectable Sas6 *(C* and *D)*. Merged images in *(B)* show Plk4 (green), Sas6 (red), and DNA (blue) stained with DAPI. *(C)* Relative fluorescence signal intensities for

centrosome-localized endogenous Plk4 were quantified from three independent experiments (≥50 cells per experiment). Bars, the mean ± standard error of the mean (SEM). *(D)* The number of centrosomal Sas6 signals per cell was quantified from three independent experiments (≥200 cells per experiment). Bars, standard deviation. *(E)* To monitor cell cycle progression, flow cytometry analysis was carried out and the results were analyzed using the ModFit LT program. Note that depleting Cep192 decreases the levels of both Plk4 and Sas6. On the other hand, depleting Cep152 rather increases the level of Plk4 at centrosomes, but greatly diminishes the level of Sas6. These somewhat unexpected observations on the levels of Plk4 in the Cep192- or Cep152-depleted cells suggest that Plk4 recruitment to centrosomes is intricately regulated through the functions of two scaffolds, Cep192 and Cep152. The results also suggest that the accumulated Plk4 in the siCep152 cells may not be competent for recruiting Sas6 and perhaps other downstream components in the absence of Cep152. Hence, Cep152 plays a key role in mediating the procentriole assembly process.

**Fig. S10.** Schematic of experimental procedures used to generate Cep192- or Cep152-expressing cells depleted of its respective endogenous protein. To stably express Cep192 or Cep152, asynchronously growing U2OS cells were infected with lentiviruses expressing RNAi-resistant, full-length (untagged) Cep192-*sil* or Cep152-*sil*, and were selected with puromycin. The cells were then depleted of endogenous Cep192 or Cep152 by siRNA transfection, and then used for various experiments shown in Fig. 5 and Figs. S11–S14.

**Fig. S11.** Centrosomal localization of exogenously expressed Cep192 and Cep152 and their respective 2A mutants. The cells obtained in Fig. 5*A* were subjected to immunostaining analyses to access the level of centrosome-localized Cep192 and Cep152 signals. *(A)* Representative images of endogenous Cep192 (siGL panel) and exogenously expressed Cep192 and its 2A mutant (siCep192 panels) are provided. Merge images show Cep192 (green) and DNA (blue) stained with DAPI. *(B)* Fluorescence intensities of centrosome-localized Cep192 signals in *(A)* were quantified from three independent experiments (≥20 cells per experiment). Bars, the mean ± standard error of the mean (SEM). Note that exogenously expressed Cep192 and its Plk4-binding-defective 2A mutant localized to centrosomes as efficiently as endogenous Cep192 (siGL panel). This finding suggests that Plk4 binding to Cep192 does not alter the capacity of Cep192 to localize to this site. *(C)* Representative images of endogenous Cep152 (siGL panel) and exogenously expressed Cep152 and its 2A mutant (siCep152 panels) are provided. Merge images show Cep152 (green) and DNA (blue) stained with DAPI. *(D)* Fluorescence intensities of centrosome-localized Cep152 signals in *(C)* were quantified from three independent experiments (≥15 cells per experiment). Bars, the mean ± standard error of the mean (SEM). Like Cep192 shown in *(A* and *B)*, exogenously expressed Cep152 and its respective 2A mutant were found to be associated with centrosomes nearly as efficiently as endogenous Cep152 (siGL panel) was.

**Fig. S12.** Ectopic expression of Cep192 or Cep152, but not its Plk4-binding-defective 2A mutant, enhances the level of centrosomal Plk4. The siGL cells in Fig. 5*A* were subjected to immunostaining analysis with an anti-Plk4 antibody. *(A)* Representative images of

centrosome-localized Plk4 (red) and DNA (blue) are shown. *(B)* Fluorescence intensities of centrosome-localized Plk4 signals were quantified from three independent experiments (≥15 cells per experiment). Bars, the mean ± standard error of the mean (SEM).

**Fig. S13.** The effect of the Cep192-Plk4 or Cep152-Plk4 interaction on the recruitment of Plk4 to centrosomes. The siCep192 (*A*) or siCep152 *(B)* cells generated in Fig. 5*A* were used to perform immunostaining analyses with an anti-Plk4 antibody. The quantification data are shown in Fig. 5*B*. Merge images show Plk4 (red) and DNA (blue) stained with DAPI. The results showed that the siCep192 cells expressing Cep192 WT, but not its Plk4-binding-defective 2A mutant, restored Plk4 localization to centrosomes (*A*). In contrast, although the siCep152 cells expressing Cep152 WT exhibited the normal level of Plk4 localized to centrosomes, the siCep152 cells expressing the Plk4-binding-defective Cep152 (2A) mutant displayed rather strongly increased Plk4 signals at centrosomes *(B)*. Representative images of centrosome-localized Plk4 in Cep192- or Cep152-expressing cells are provided.

**Fig. S14.** Loss of either the Cep192- or Cep152-dependent interaction with Plk4 is sufficient to impair Sas6 recruitment to centrosomes. (*A* and *B*) Representative images are provided. Merge images show Sas6 (red) and DNA (blue) stained with DAPI. The quantification data are shown in Fig. 5*E*.

**Fig. S15.** The Cep152-Plk4 complex, but not the Cep192-Plk4 complex, interacts with Cep135. 293T cells cotransfected with the indicated constructs were subjected to

immunoprecipitation (IP) analysis with anti-FLAG antibody. "-" indicates control vector. *(A)* Immunoprecipitation of Sas6 failed to detectably coprecipitate Cep192 or Cep152 regardless of the presence or absence of Plk4. *(B)* 293T cells cotransfected with the indicated constructs were subjected to immunoprecipitation (IP) analysis with anti-FLAG antibody. Note that Cep135 efficiently coprecipitated both Cep152 and Plk4, whereas it failed to co-precipitate Cep192. These data suggest that the Cep152-Plk4 complex, but not the Cep192-Plk4 complex, directly interacts with downstream components, such as Cep135, to induce centriole biogenesis.

## Supplemental References


1. Lee, K. S., Yuan, Y. -L., Kuriyama, R., & Erikson, R. L. Plk is an M-phase-specific protein kinase and interacts with a kinesin-like protein, CHO1/MKLP-1. *Mol. Cell. Biol.* **15**, 7143-7151 (1995).
2. Johmura, Y.*, et al.* Regulation of microtubule-based microtubule nucleation by mammalian polo-like kinase 1. *Proc. Natl. Acad. Sci. USA.* **108**, 11446-11451 (2011).
3. Kang, Y. H.*, et al.* Self-regulation of Plk1 recruitment to the kinetochores is critical for chromosome congression and spindle checkpoint signaling. *Mol. Cell* **24**, 409-422 (2006).
4. Elbashir, S. M.*, et al.* Duplexes of 21-nucleotide RNAs mediate RNA interference in cultured mammalian cells. *Nature.* **411**, 494-498 (2001).
5. Cizmecioglu, O.*, et al.* Cep152 acts as a scaffold for recruitment of Plk4 and CPAP to the centrosome. *J. Cell Biol.* **191**, 731-739 (2010).

**Fig. S1**

**A**

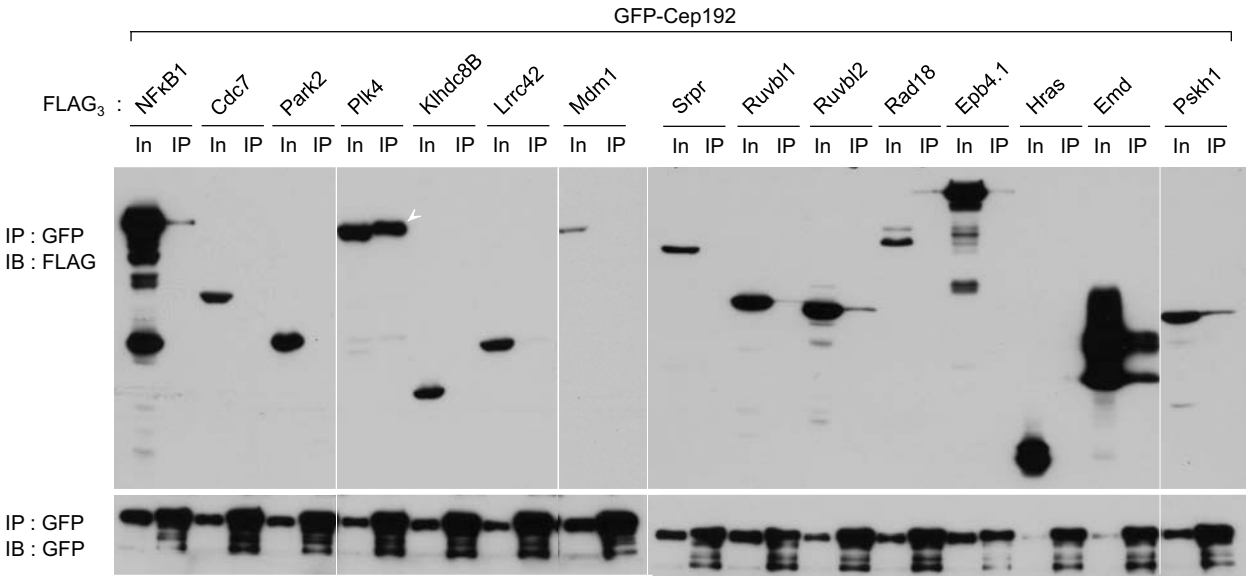
GFP-Cep192
FLAG3 :
NFκB1
Cdc7
Park2
Plk4
Klhdc8B
Lrrc42
Mdm1
Srpr
Ruvbl1
Ruvbl2
Rad18
Epb4.1
Hras
Emd
Pskh1
In IP
IP : GFP
IB : FLAG
IP : GFP
IB : GFP

**B**

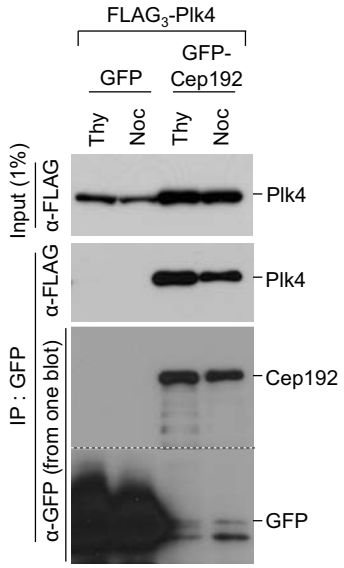
FLAG3-Plk4
GFP
GFP-Cep192
Thy
Noc
Thy
Noc
Input (1%)
α-FLAG
Plk4
IP : GFP
α-FLAG
Plk4
α-GFP (from one blot)
Cep192
GFP

**Fig. S2**

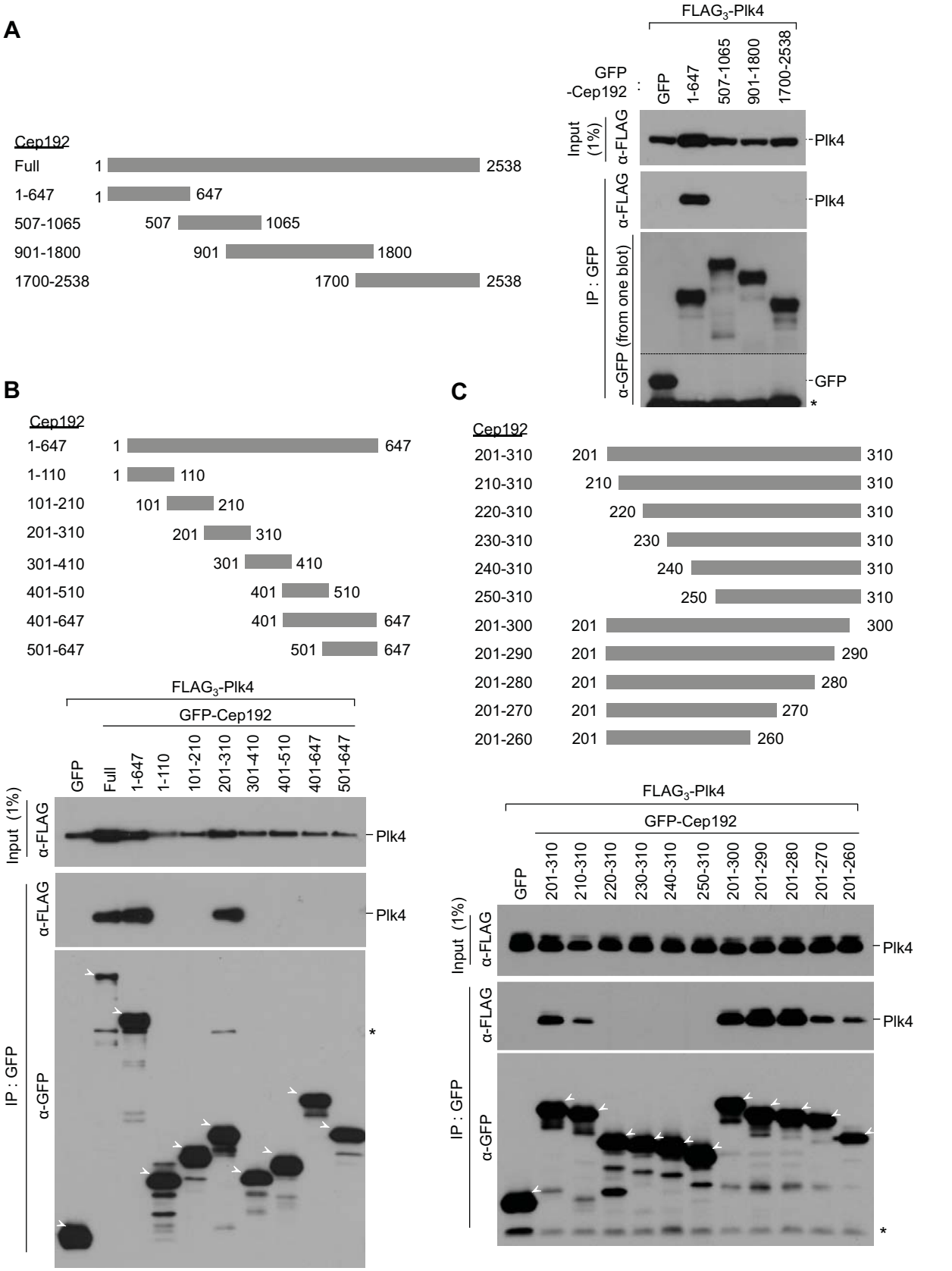
A
Cep192
Full 1 2538
1-647 1 647
507-1065 507 1065
901-1800 901 1800
1700-2538 1700 2538
FLAG3-Plk4
GFP -Cep192 : GFP 1-647 507-1065 901-1800 1700-2538
Input (1%) α-FLAG
IP : GFP α-FLAG
α-GFP (from one blot)
Plk4
GFP
*
B
Cep192
1-647 1 647
1-110 1 110
101-210 101 210
201-310 201 310
301-410 301 410
401-510 401 510
401-647 401 647
501-647 501 647
FLAG3-Plk4
GFP-Cep192
GFP Full 1-647 1-110 101-210 201-310 301-410 401-510 401-647 501-647
Input (1%) α-FLAG
IP : GFP α-FLAG
α-GFP
Plk4
*
C
Cep192
201-310 201 310
210-310 210 310
220-310 220 310
230-310 230 310
240-310 240 310
250-310 250 310
201-300 201 300
201-290 201 290
201-280 201 280
201-270 201 270
201-260 201 260
FLAG3-Plk4
GFP-Cep192
GFP 201-310 210-310 220-310 230-310 240-310 250-310 201-300 201-290 201-280 201-270 201-260
Input (1%) α-FLAG
IP : GFP α-FLAG
α-GFP
Plk4
*

Fig. S3

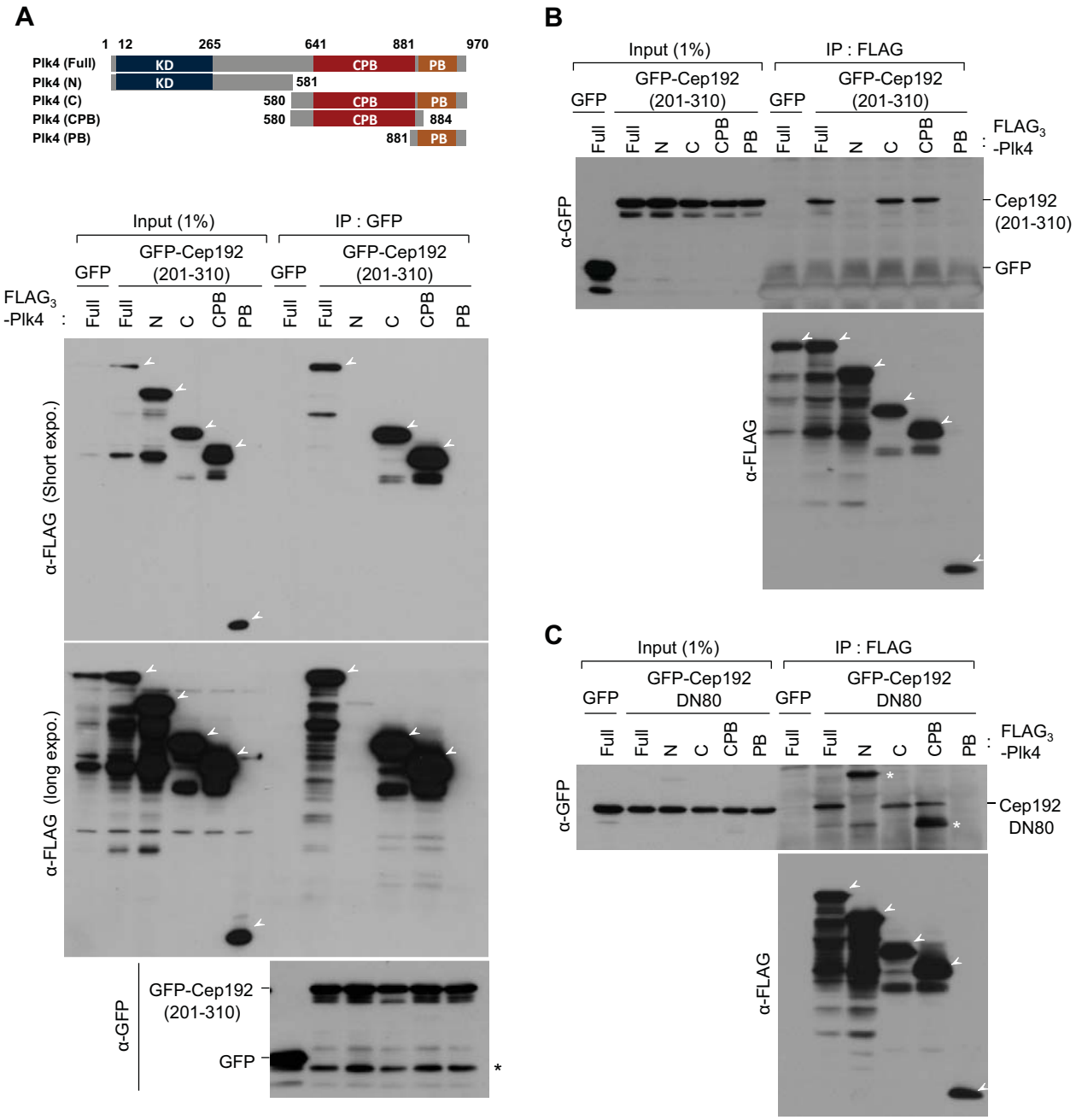
A
1 12 265 641 881 970
Plk4 (Full)
Plk4 (N)
Plk4 (C)
Plk4 (CPB)
Plk4 (PB)
KD
CPB
PB
581
580
884
881
Input (1%)
IP : GFP
GFP
GFP-Cep192 (201-310)
FLAG3 -Plk4 :
Full
N
C
CPB
PB
α-FLAG (Short expo.)
α-FLAG (long expo.)
α-GFP
GFP-Cep192 (201-310)
GFP
*
B
Input (1%)
IP : FLAG
GFP
GFP-Cep192 (201-310)
FLAG3 -Plk4 :
α-GFP
Cep192 (201-310)
GFP
α-FLAG
C
Input (1%)
IP : FLAG
GFP
GFP-Cep192 DN80
FLAG3 -Plk4 :
α-GFP
Cep192 DN80
α-FLAG

**Fig. S4**

**Cep192 DN80**

**Acidic-α-helix** **N/Q-rich motif**

201- EKLILPTSLEDSSDDDIDDEMFYDDHLEAYFEQLAIPGMIYEDLEGPEPPEKGFKLPTNGLRQANENGSLNCKFQSENNS -280

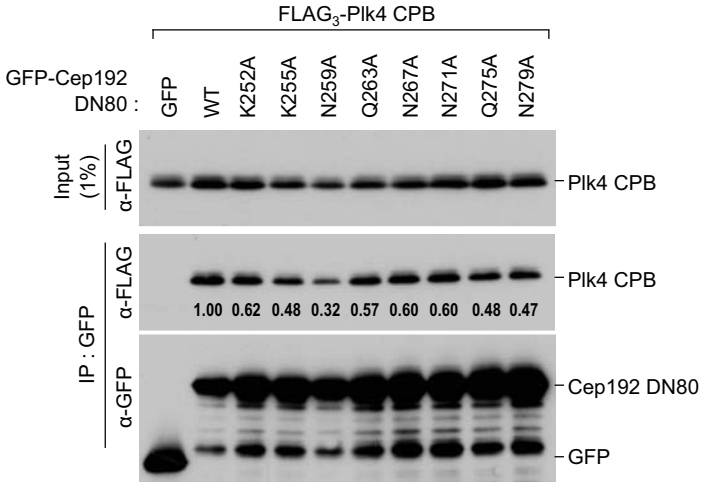

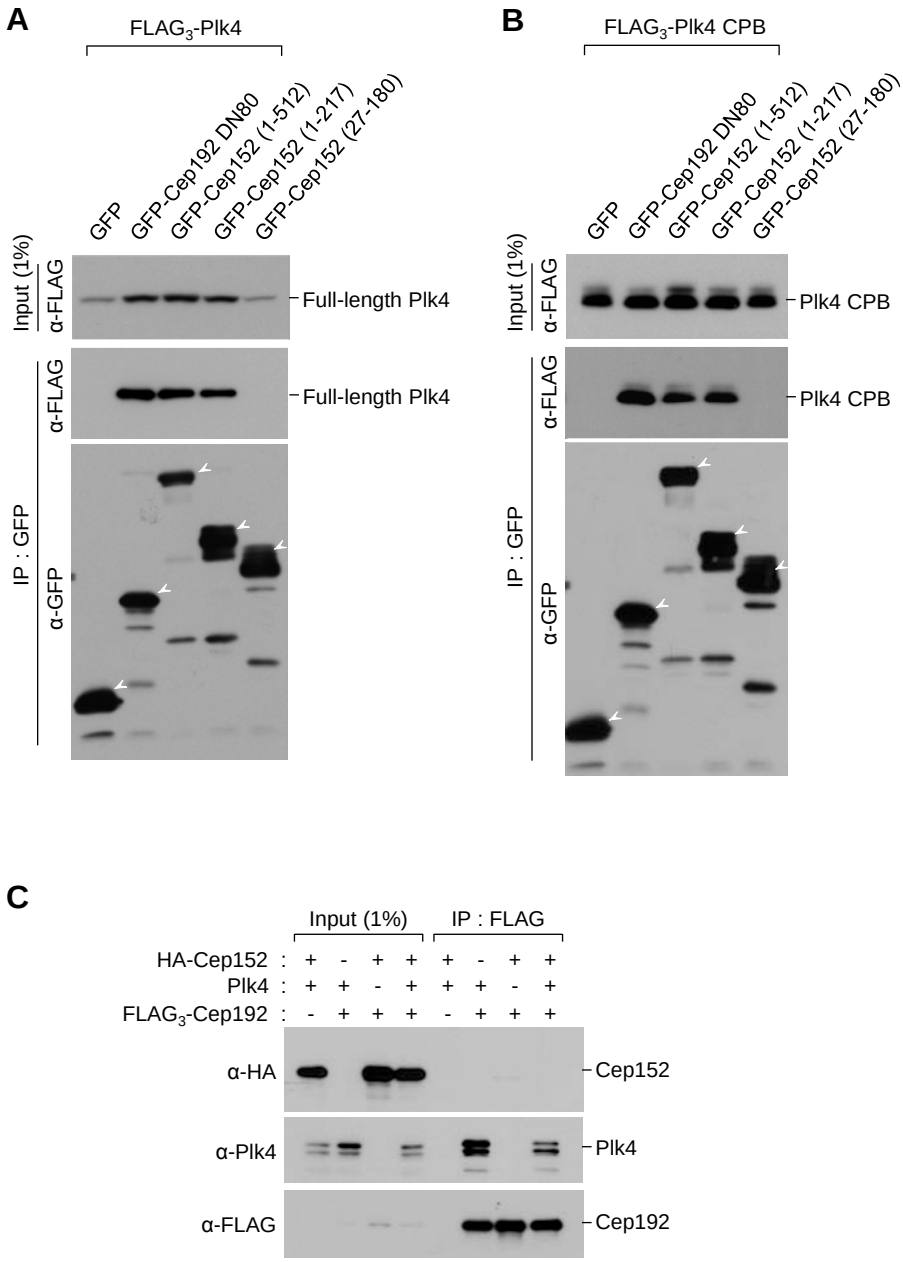
A
FLAG3-Plk4
GFP
GFP-Cep192 DN80
GFP-Cep152 (1-512)
GFP-Cep152 (1-217)
GFP-Cep152 (27-180)
Input (1%)
α-FLAG
Full-length Plk4
IP : GFP
α-FLAG
Full-length Plk4
α-GFP
B
FLAG3-Plk4 CPB
GFP
GFP-Cep192 DN80
GFP-Cep152 (1-512)
GFP-Cep152 (1-217)
GFP-Cep152 (27-180)
Input (1%)
α-FLAG
Plk4 CPB
IP : GFP
α-FLAG
Plk4 CPB
α-GFP
C
Input (1%)
IP : FLAG
HA-Cep152 : + - + + + - + +
Plk4 : + + - + + + - +
FLAG3-Cep192 : - + + + - + + +
α-HA
Cep152
α-Plk4
Plk4
α-FLAG
Cep192

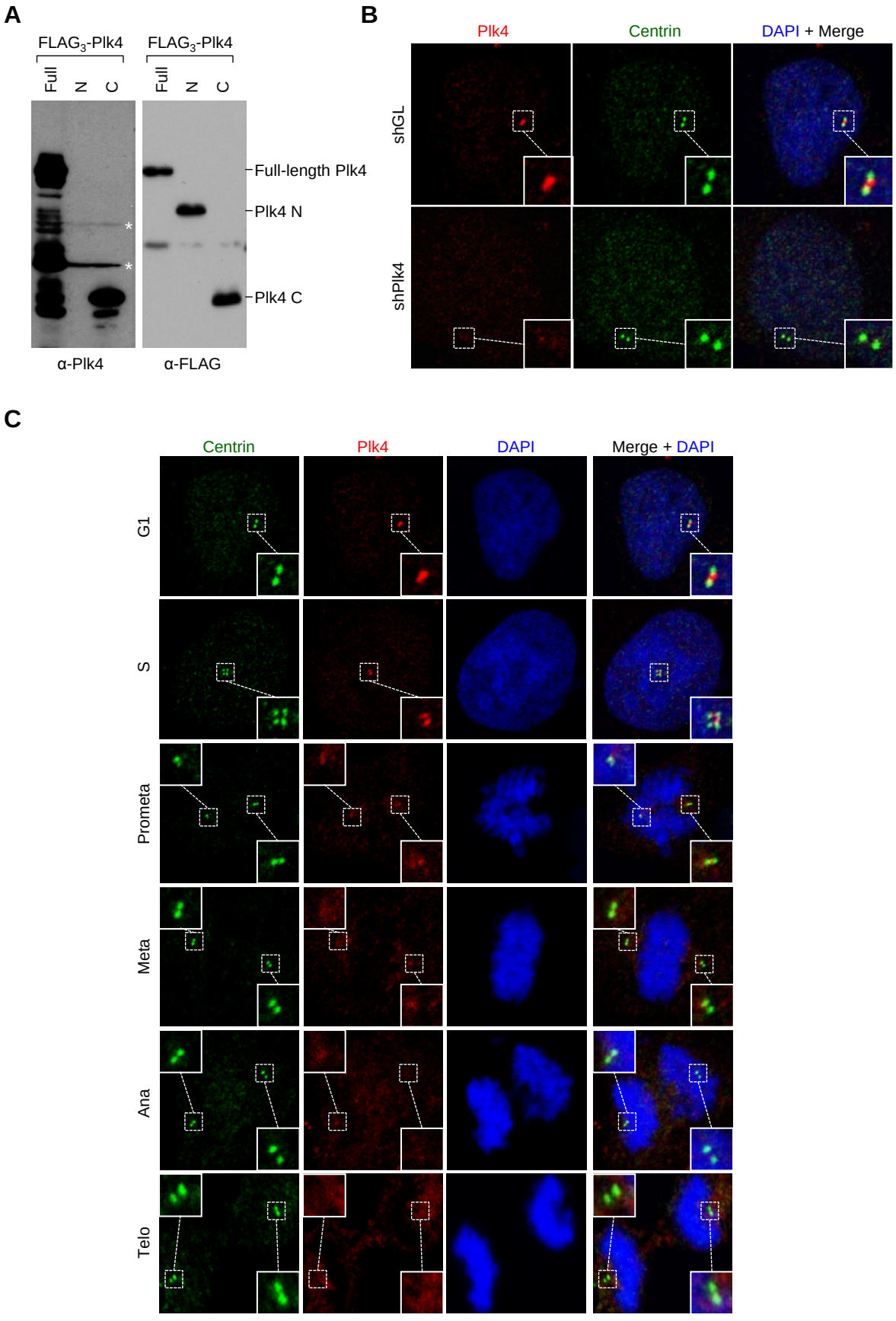
A
FLAG3-Plk4
FLAG3-Plk4
Full
N
C
Full
N
C
Full-length Plk4
Plk4 N
Plk4 C
α-Plk4
α-FLAG
B
Plk4
Centrin
DAPI + Merge
shGL
shPlk4
C
Centrin
Plk4
DAPI
Merge + DAPI
G1
S
Prometa
Meta
Ana
Telo

**Fig. S7**

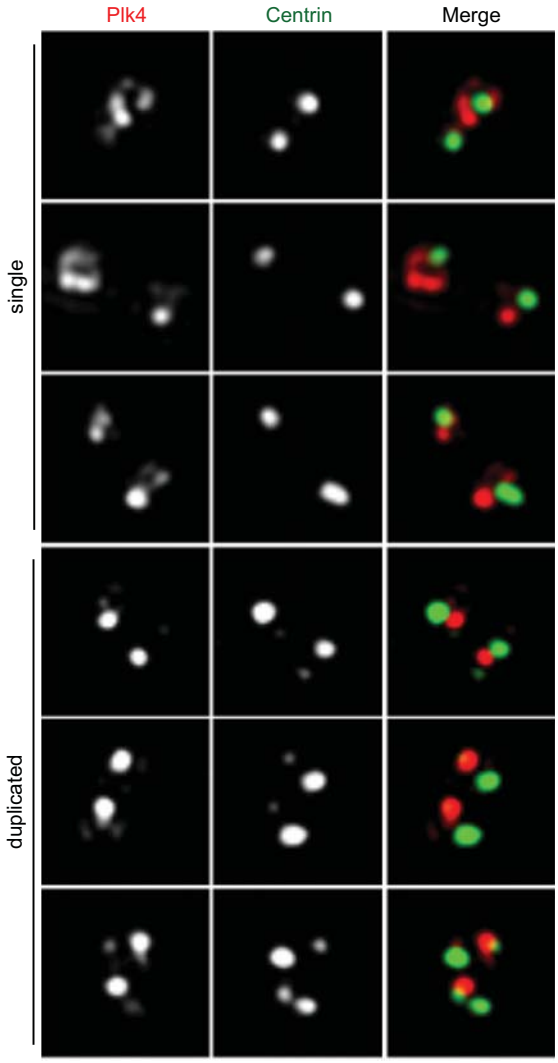

Fig. S8

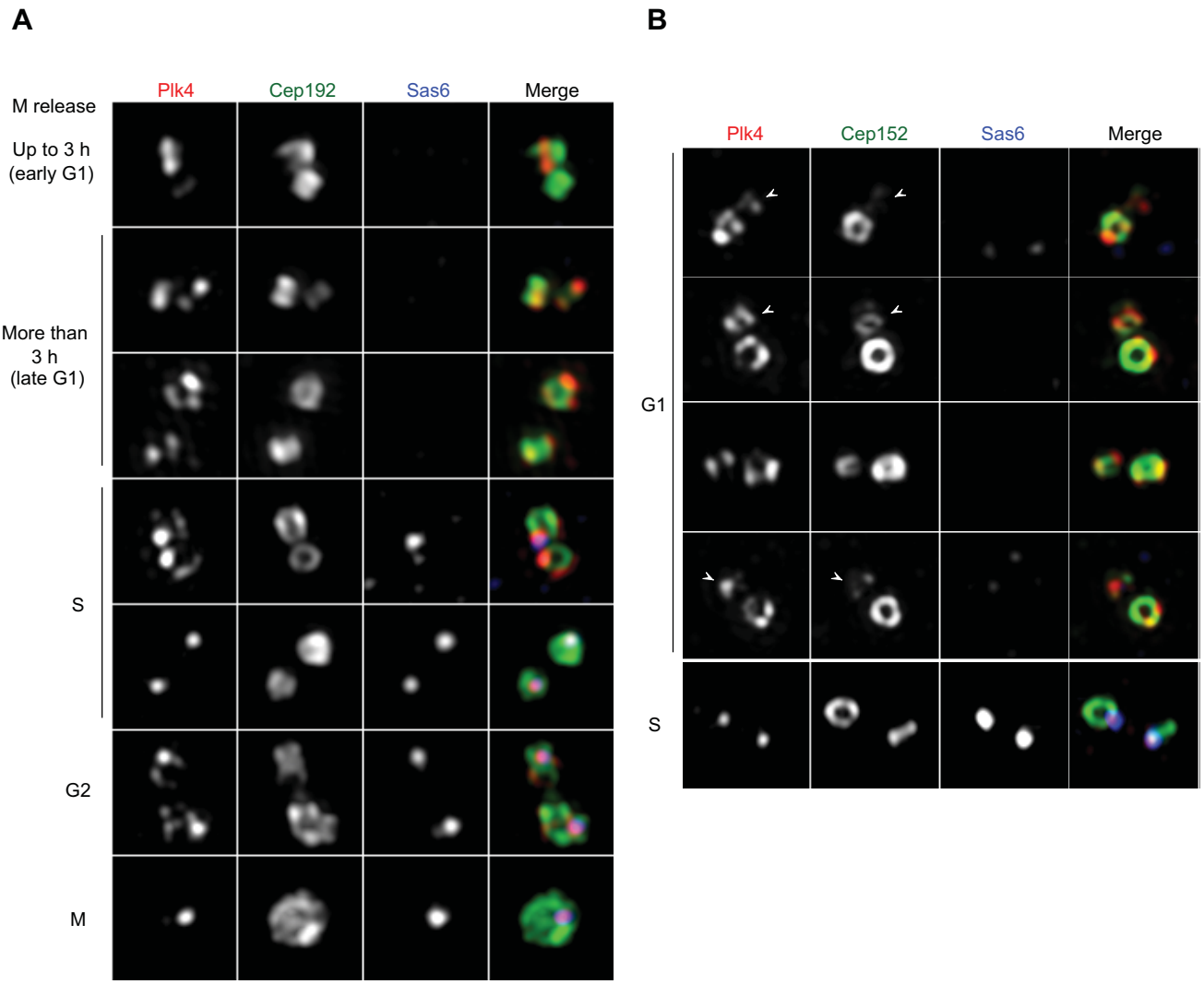
A
Plk4
Cep192
Sas6
Merge
M release
Up to 3 h
(early G1)
More than
3 h
(late G1)
S
G2
M
B
Plk4
Cep152
Sas6
Merge
G1
S

Fig. S9

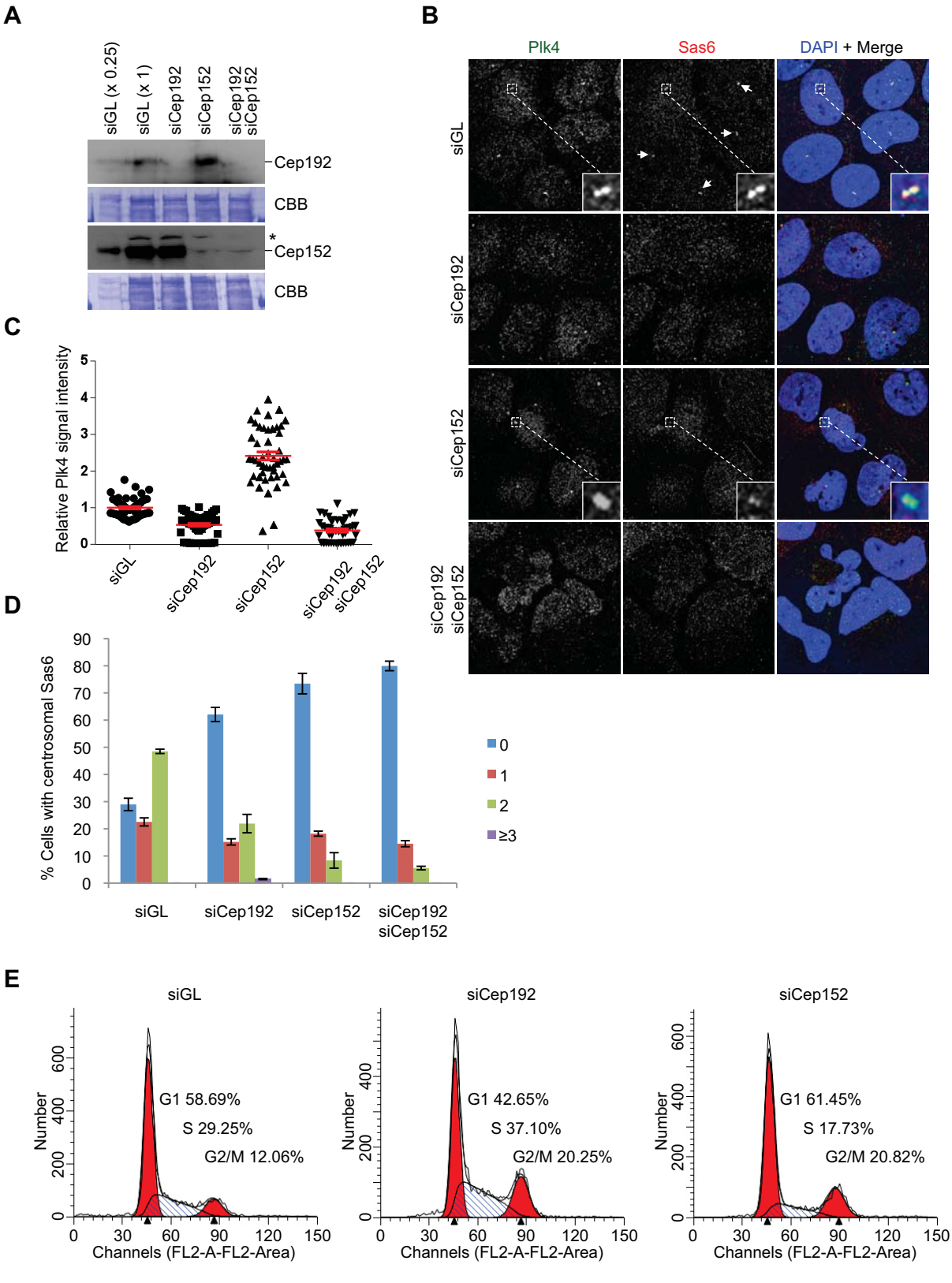
A
siGL (x 0.25)
siGL (x 1)
siCep192
siCep152
siCep192 siCep152
Cep192
CBB
*
Cep152
CBB
B
Plk4
Sas6
DAPI + Merge
siGL
siCep192
siCep152
siCep192 siCep152
C
Relative Plk4 signal intensity
0
1
2
3
4
5
siGL
siCep192
siCep152
siCep192 siCep152
D
% Cells with centrosomal Sas6
0
10
20
30
40
50
60
70
80
90
siGL
siCep192
siCep152
siCep192 siCep152
0
1
2
≥3
E
siGL
G1 58.69%
S 29.25%
G2/M 12.06%
siCep192
G1 42.65%
S 37.10%
G2/M 20.25%
siCep152
G1 61.45%
S 17.73%
G2/M 20.82%
Number
0
200
400
600
0
30
60
90
120
150
Channels (FL2-A-FL2-Area)

**Fig. S10**

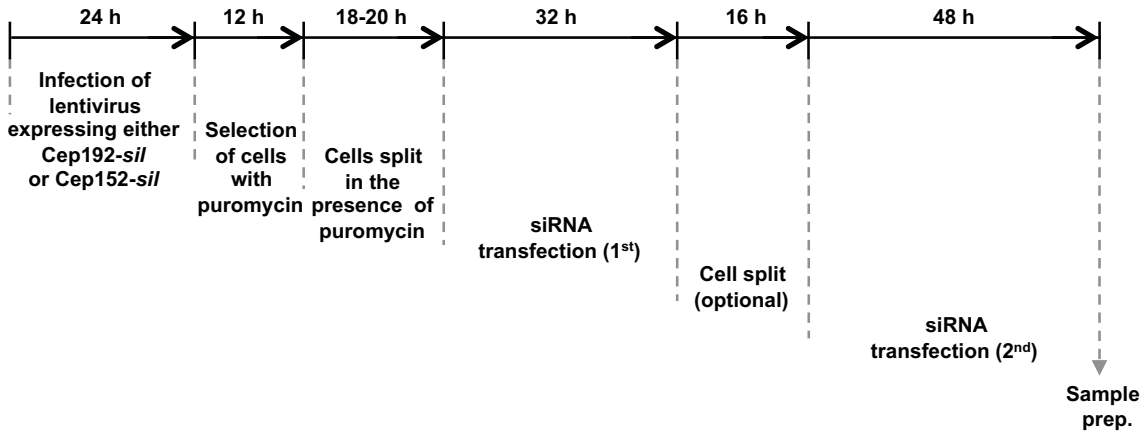
24 h
12 h
18-20 h
32 h
16 h
48 h
Infection of lentivirus expressing either Cep192-*siI* or Cep152-*siI*
Selection of cells with puromycin
Cells split in the presence of puromycin
siRNA transfection (1st)
Cell split (optional)
siRNA transfection (2nd)
Sample prep.

Fig. S11

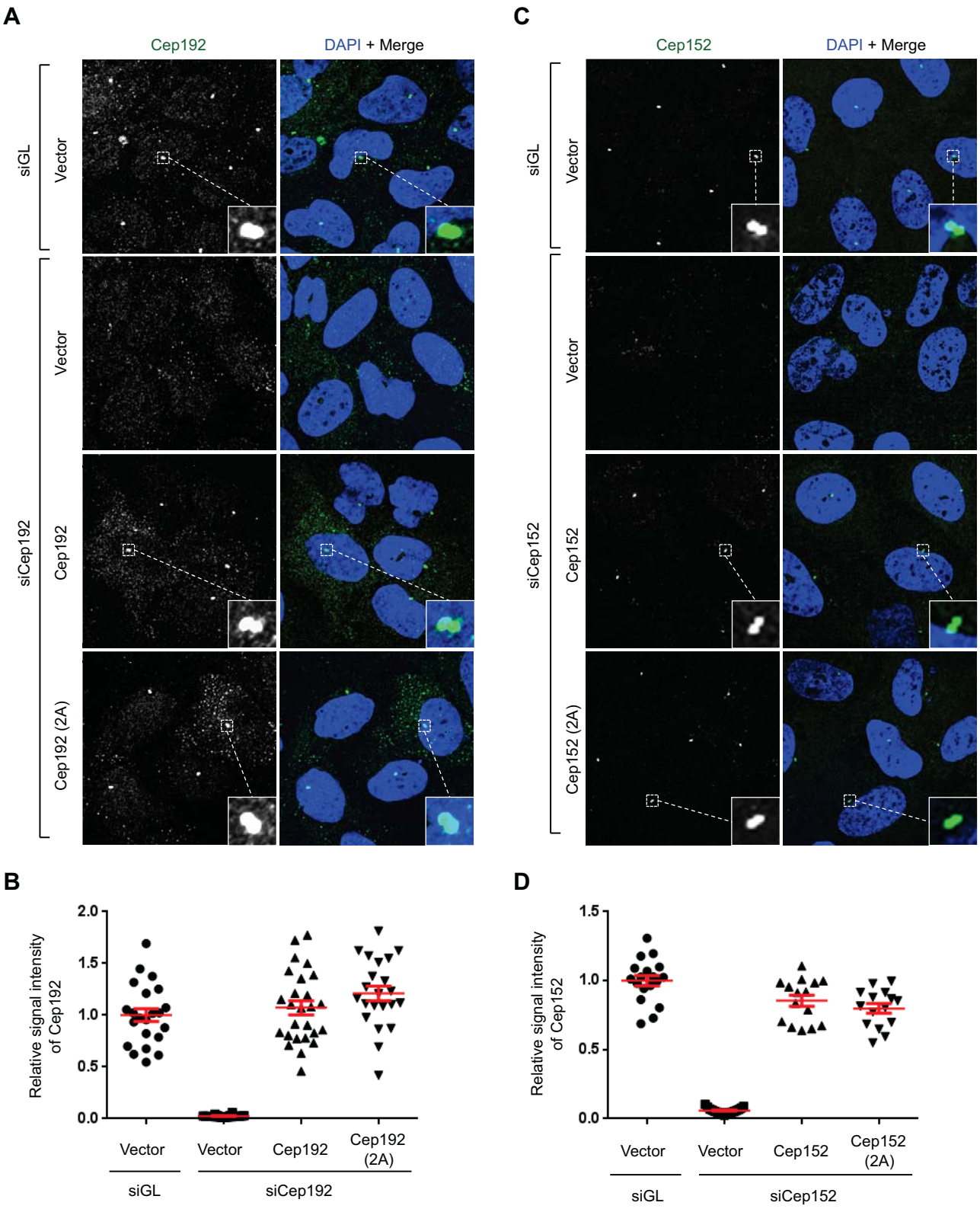
A
Cep192
DAPI + Merge
siGL
Vector
siCep192
Vector
Cep192
Cep192 (2A)
C
Cep152
DAPI + Merge
siGL
Vector
siCep152
Vector
Cep152
Cep152 (2A)
B
Relative signal intensity of Cep192
2.0
1.5
1.0
0.5
0.0
Vector
Vector
Cep192
Cep192 (2A)
siGL
siCep192
D
Relative signal intensity of Cep152
1.5
1.0
0.5
0.0
Vector
Vector
Cep152
Cep152 (2A)
siGL
siCep152

Fig. S12

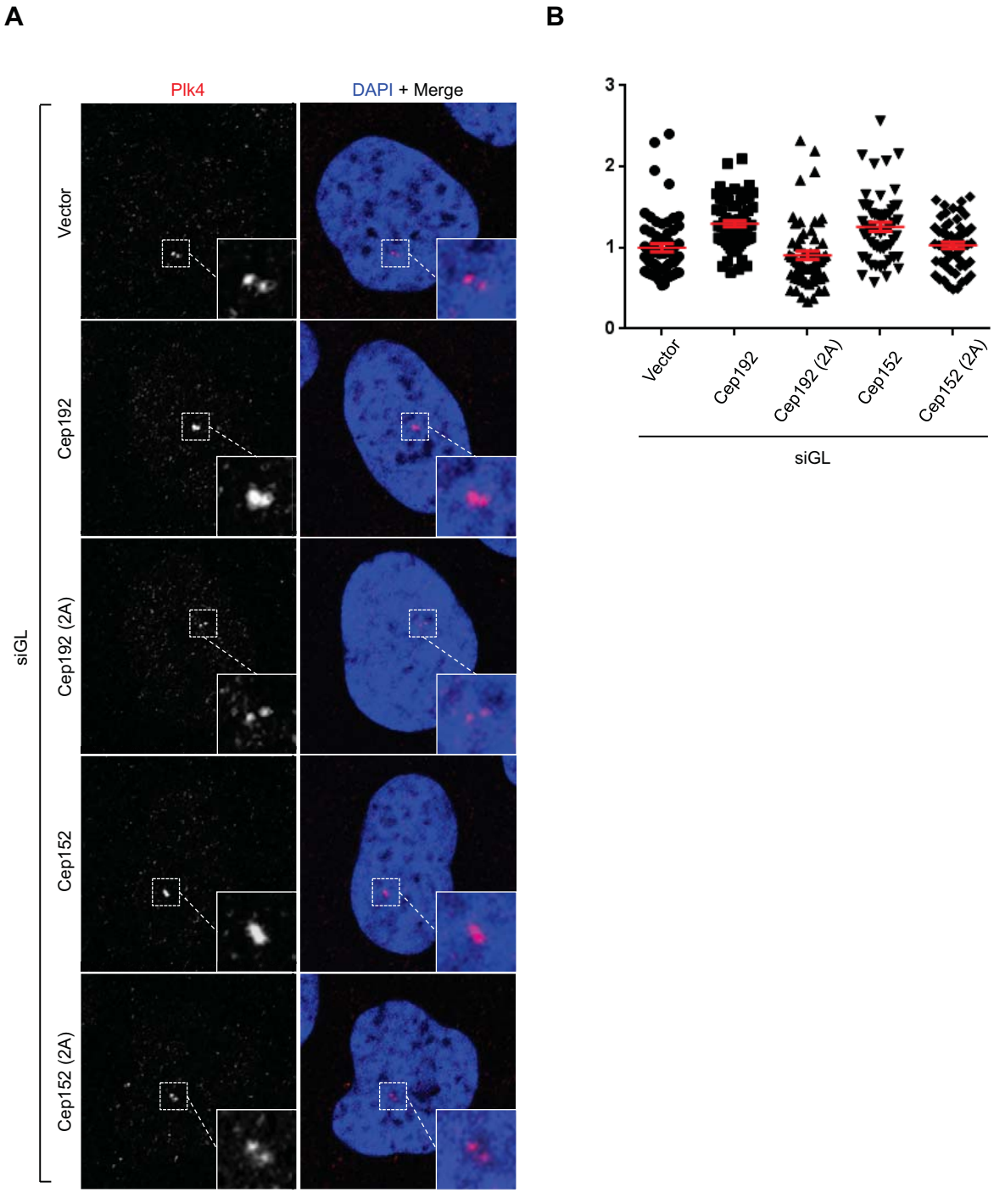
A
Plk4
DAPI + Merge
siGL
Vector
Cep192
Cep192 (2A)
Cep152
Cep152 (2A)
B
3
2
1
0
Vector
Cep192
Cep192 (2A)
Cep152
Cep152 (2A)
siGL

Fig. S13

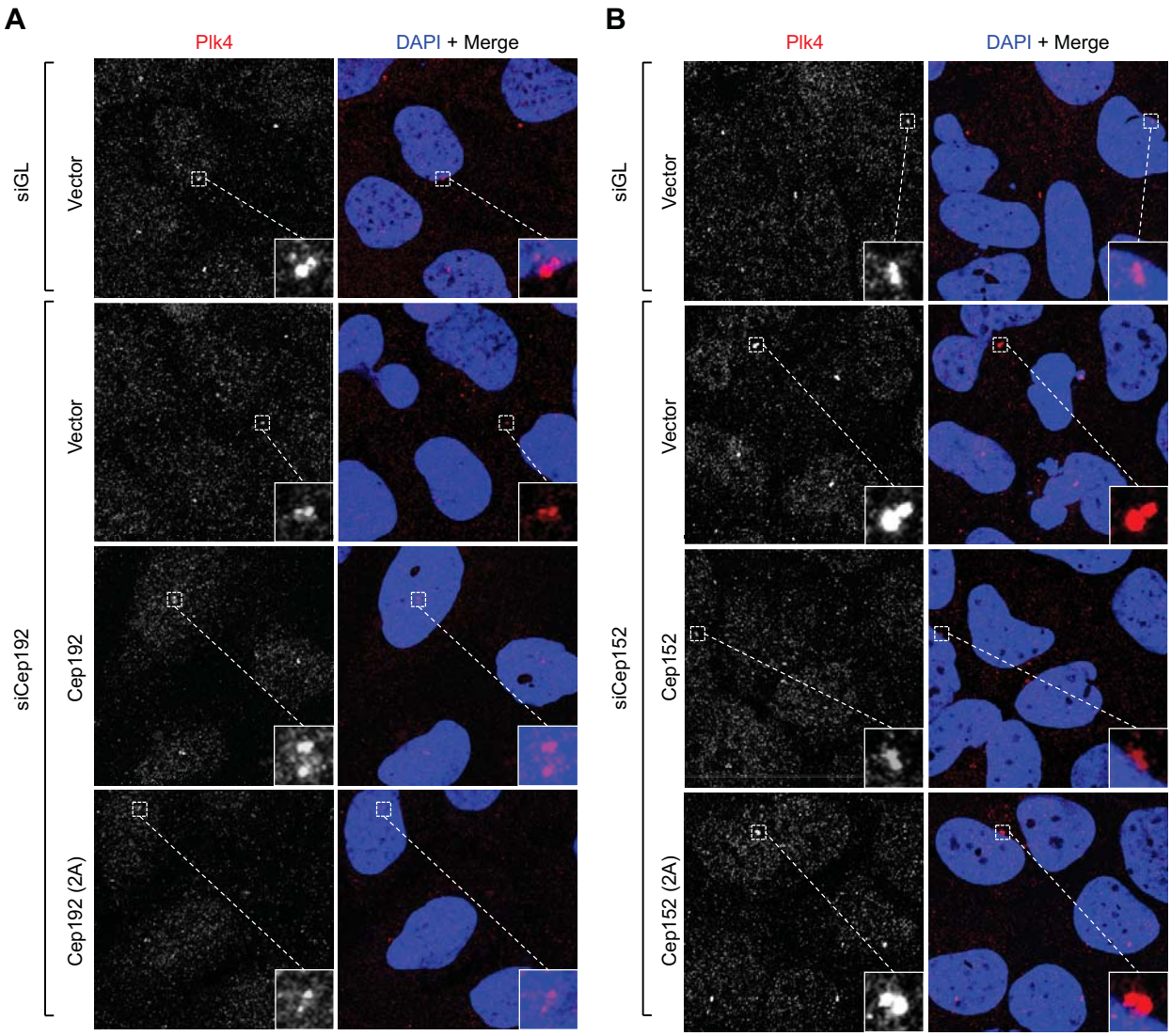
A
Plk4
DAPI + Merge
siGL
Vector
siCep192
Vector
Cep192
Cep192 (2A)
B
Plk4
DAPI + Merge
siGL
Vector
siCep152
Vector
Cep152
Cep152 (2A)

Fig. S14

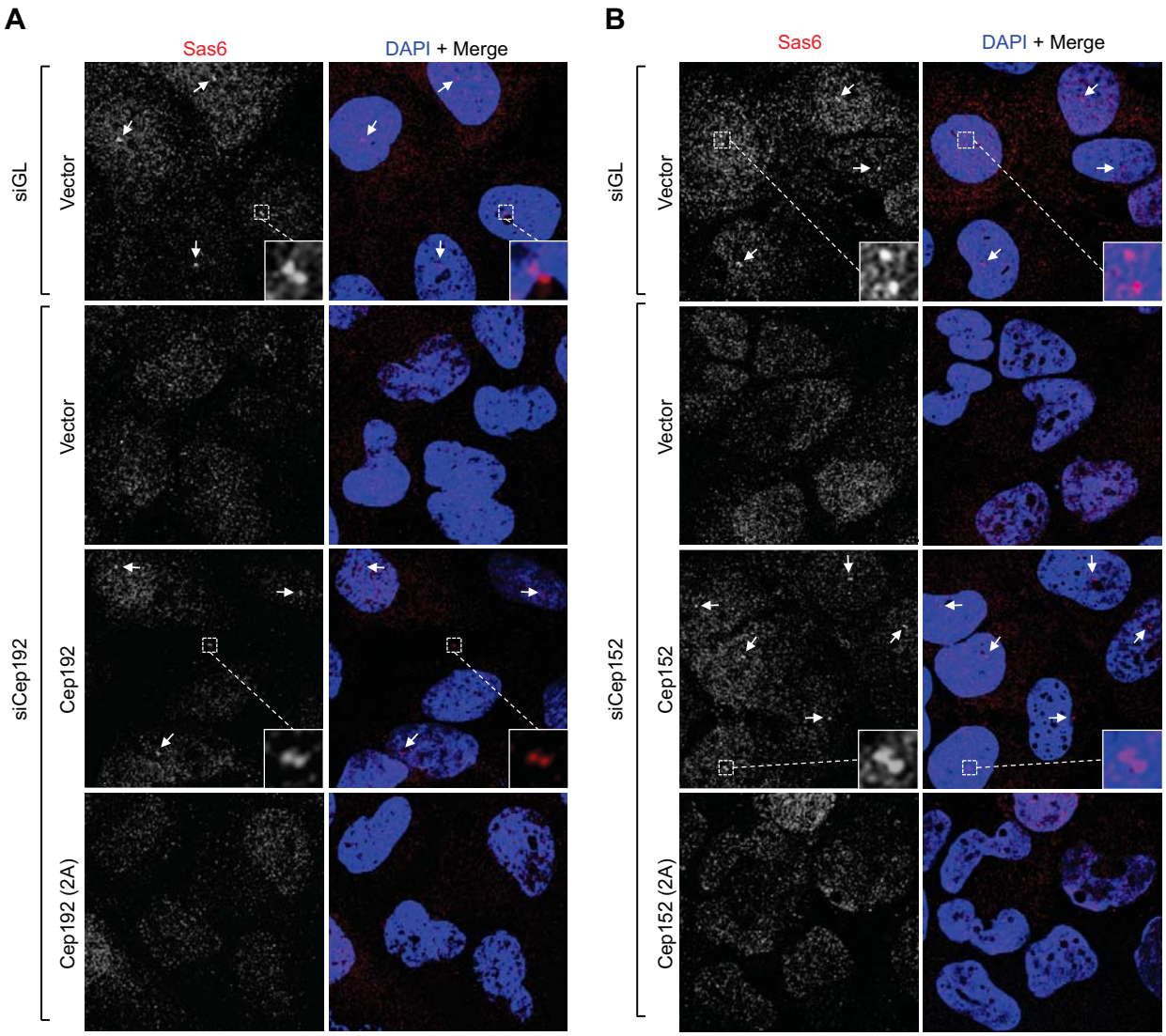
A
Sas6
DAPI + Merge
siGL
Vector
siCep192
Vector
Cep192
Cep192 (2A)
B
Sas6
DAPI + Merge
siGL
Vector
siCep152
Vector
Cep152
Cep152 (2A)

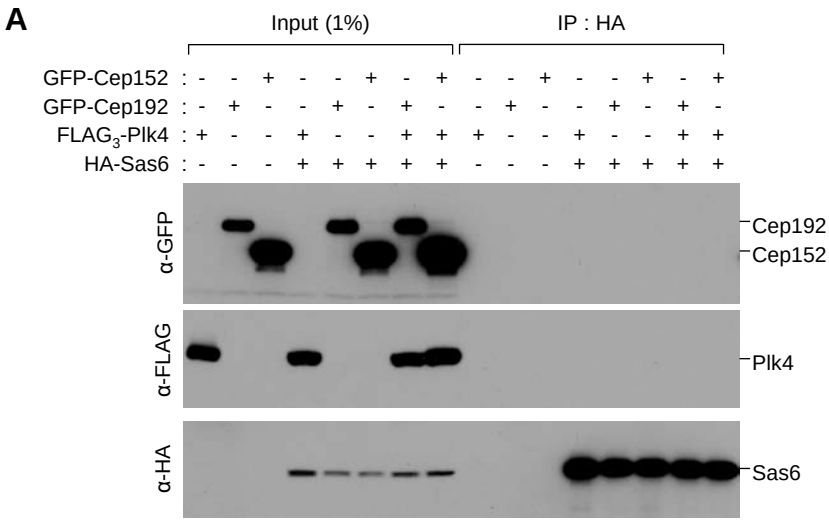
A
Input (1%)
IP : HA
GFP-Cep152 : - - + - - + - + - - + - - + - +
GFP-Cep192 : - + - - + - + - - + - - + - + -
FLAG3-Plk4 : + - - + - - + + + - - + - - + +
HA-Sas6 : - - - + + + + + - - - + + + + +
α-GFP
α-FLAG
α-HA
Cep192
Cep152
Plk4
Sas6

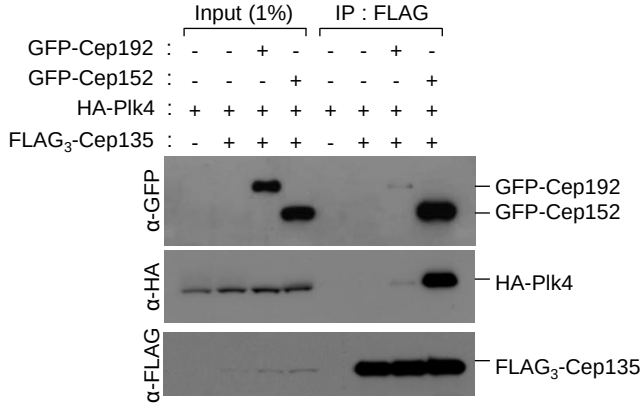
B
Input (1%)
IP : FLAG
GFP-Cep192 : - - + - - - + -
GFP-Cep152 : - - - + - - - +
HA-Plk4 : + + + + + + + +
FLAG3-Cep135 : - + + + - + + +
α-GFP
α-HA
α-FLAG
GFP-Cep192
GFP-Cep152
HA-Plk4
FLAG3-Cep135

**Table S1. siRNA sequences used in this study**

| Target gene | Sequence (nt positions from the start codon) | Reference | Type |
|---|---|---|---|
| Luciferase | CGTACGCGGAATACTTCGA | (4 ) | lentivirus, synthetic |
| Cep192 | GCTAGTATGTCTGATACTTGG (2407-2427) | This study | lentivirus, synthetic |
| Cep152 | GCGGATCCAACTGGAAATCTA (3099-4019) | (5) | lentivirus, synthetic |
| Cep152 | GGTTTGGAACCGTATAATA (556-574) | This study | lentivirus |
| Plk4 (3'UTR) | CAGTGTCTGATGAAACATT (3626-3645) | This study | lentivirus, synthetic |

**Table S2. Antibodies used in this study**

| Antibodies | Species | Source |
|---|---|---|
| Anti-Cep192 (1-647) | Rabbit | This study |
| Anti-Cep192 (201-280) | Rabbit | This study |
| Anti-Cep152 (491-810) | Rabbit | This study |
| Anti-Cep152 (31-46) | Rabbit | This study |
| Anti-Plk4 (580-970) | Rabbit | This study |
| Anti-Plk1 | Mouse | Santa Cruz Biotechnologies, Santa Cruz, CA |
| Anti-GFP | Rabbit | Santa Cruz Biotechnologies, Santa Cruz, CA |
| Anti-FLAG | Mouse | Sigma, St. Louis, MO |
| Anti-HA | Rat | Roche, Mannheim, Germany |
| Anti-Sas6 | Mouse | Santa Cruz Biotechnologies, Santa Cruz, CA |
| Anti-Centrin | Mouse | Millipore, Billerica, MA |